Optics Communications 283 (2010) 4582–4585

Contents lists available at ScienceDirect

Optics Communications

journal homepage: www.elsevier.com/locate/optcom

Artifactual circular dichroism effect in a photoelastic modulator

Y.F. Chao, P.L. Lin *

Department of Photonics & Institute of Electro-Optical Engineering, No.1001, University Rd. Hsinchu , Taiwan

ARTICLE INFO

Article history:
Received 21 December 2009
Received in revised form 26 June 2010
Accepted 30 June 2010

ABSTRACT

The three-intensity technique is used to calibrate a photoelastic modulator by its temporal waveform. This method not only allows us to measure the intrinsic static phase retardation and modulation amplitude but also provides the evidence for the existence of circular dichroism (CD) in the photoelastic modulator. In this report, we will demonstrate the averaged intensity for normalization in this PEM modulated light not only depicts a periodic modulation, it also exhibits anti-symmetric distributions at $P=45°$ and $P=-45°$, which was considered as constant for conventional PEM ellipsometry. Four models were examined to verify that only a circular dichroism medium coupled with the periodical induced birefringence modulator can explain the phenomena. This work can quantitatively measure the artifactual CD effect of PEM and reduce its system error in CD spectrometer which consists of a PEM.

1. Introduction

The photoelastic modulator (PEM) is a device that uses the photoelastic effect to modulate phase retardation harmonically [1]. Recently, the PEM has been used to replace the wave plate in some metrological techniques, especially for polarization-related measurements [2]. To ensure optimum performance, it is necessary to accurately calibrate the azimuth angle, initial static retardation and modulation amplitude of the PEM. Using data acquisition (DAQ) system, Wang et al. [3] carefully determined the modulation amplitude by its digitized temporal waveform. The three-intensity measurement technique [4] in a polarizer–PEM–analyzer configuration is used as another alternative method to calibrate the photoelastic modulator through its temporal waveform. To our surprise, its asymmetric intensity distribution at $P=-45°$ and 45° can only be explained by the existence of circular dichroism (CD) in the PEM. Because of the existence of this artifactual CD, Claborn et al. [5] constructed a new circular dichroism imaging microscopy instead of using a commercial JASCO old product. In addition, Shindo [6] also showed the artifactual CD effects in the commercial CD spectrometers, both of which consist with a PEM. In fact, as early as 1972, Nordén and Davidson [7,8] had already shown that the strain in polyethylene could generate circular dichroism. The artifactual CD coupled with linear birefringence (LB) was also widely discussed by Schellman [9]. However, this effect has never been considered in the conventional PEM ellipsometry/polarimetry because only harmonics were used to deduce the physical parameters. The intensity fluctuation in DC for normalization has been averaged out in the process of measurement.

The three-intensity measurement in ellipsometry [4] has been developed to replace the over determination technique for fast Fourier transformation or least squares fit. Chao et al. [4] proved that this technique can save both time and memory without degrade the ellipsometric measurements. Moreover, this technique also provides the feasibility of establishing the two-dimensional ellipsometry/polarimetry [10–12]. Based on this concept, Han and Chao [13] also developed a stroboscopic illumination technique in the PEM modulated ellipsometry to form an imaging system. Since only four specific polarization states in a cycle were used to obtain the ellipsometric parameters, its initial phase and the stability of intensity for normalization are crucial for this technique to obtain the accurate result. This work not only can improve the measurements of PEM imaging ellipsometry/polarimetry, it also can reduce the system error in PEM-related CD measurements.

The combination of a circular diattenuator and a linear retarder is considered to be the physical model of the PEM in this work. Since the Stokes parameters can also be obtained by the same three-intensity measurements, we will investigate the state of polarization (SOP) and its angular deviation from various models on Poincare sphere.

2. Theoretical background

The basic setup for measuring the parameters of PEM is shown in Fig. 1. The Stokes vector S represents the polarization state, where subscripts f and i represent for the final and initial linear polarized states, respectively. The P-PEM-A polarimetric system can be expressed as:

$$S_f = M_A(2A)M_R(-2\theta)M_{\mathrm{PEM}}M_R(2\theta)S_i \quad (1)$$

* Corresponding author. Te1.: +886 3 5712121 31941.
E-mail address: polo_625@yahoo.com.tw (P.L. Lin).

0030-4018/$ – see front matter © 2010 Elsevier B.V. All rights reserved.
doi:10.1016/j.optcom.2010.06.096

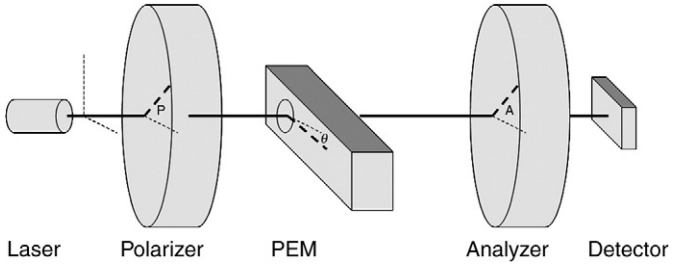

Fig. 1. Schematic setup of the polarimeter for calibrating the photoelastic modulator.

where $M_R(2\theta)$ and $M_A(2A)$ are the Mueller matrices for a rotator with rotating angle θ and an analyzer with its transmission axis at$A$, respectively. Let PEM be a combination of a diattenuator (linear dichroism M_{LD} or circular dichroism M_{CD}) and a linear retarder. All their Mueller matrices are listed in the Appendix. The four possible models of PEM are (1) $M_{LD}\,M_{LB}$, (2) $M_{LB}\,M_{LD}$, (3) $M_{LB}\,M_{CD}$ and (4) $M_{CD}\,M_{LB}$. When S_i is the linear polarized light whose azimuth is at P, the measured intensity for the above four cases can be written as

$$\begin{aligned} I_1(A) = I_2(A) = I_0[&\cosh \mathrm{LD} + \cos(2A-2\theta)\cos(2P-2\theta)\cosh \mathrm{LD} \\ &+ \cos\phi \sin(2A-2\theta)\sin(2P-2\theta) \\ &+ 2\cos(\mathrm{P}-\theta)\cos(A+P-2\theta)\sinh \mathrm{LD}], \end{aligned} \tag{2}$$

$$\begin{aligned} I_3(A) = I_0[&\cosh \mathrm{CD} + \cos(2A-2\theta)\cos(2P-2\theta) \\ &+ \cos\phi \sin(2A-2\theta)\sin(2P-2\theta) + \sin(2\mathrm{A}-2\theta)\sin\phi \sinh \mathrm{CD}], \end{aligned} \tag{3}$$

and

$$\begin{aligned} I_4(A) = I_0[&\cosh \mathrm{CD} + \cos(2A-2\theta)\cos(2P-2\theta) \\ &+ \cos\phi \sin(2A-2\theta)\sin(2P-2\theta) - \sin(2\mathrm{P}-2\theta)\sin\phi \sinh \mathrm{CD}], \end{aligned} \tag{4}$$

where I_0 is the normalized intensity and φ *is* the phase retardation of linear retarder. The averaged intensity measured by the three intensities at the azimuth of the analyzer at 0°, 60° and 120° is noted as I_{ki} ,

$$I_{ki} = \frac{1}{3}\left[I_i(0) + I_i\left(\frac{\pi}{3}\right) + I_i\left(\frac{2\pi}{3}\right)\right] \tag{5}$$

and i indicates the case number, it is easy to prove

$$I_{k1} = I_{k2} = I_0[\cosh \mathrm{LD} + \cos(2P-\theta)\sinh \mathrm{LD}], \tag{6}$$

$$I_{k3} = I_0 \cosh \mathrm{CD}. \tag{7}$$

From Eq. (7), one can immediately conclude that I_{k3} is static; moreover, when $P=\pm 45^{\circ}$and θ of PEM is close zero (see Eq. (6)), both I_{k1} and I_{k2} are also independent of the modulated phase ϕ. None of these three cases exhibit the observed asymmetric intensity distribution at $P=-45°$ and 45°. However, the averaged intensity I_{k4},

$$I_{k4} = I_0[\cosh \mathrm{CD} - \sin(2P-\theta)\sin\phi \sinh \mathrm{CD}], \tag{8}$$

presents a periodical distribution under the phase modulation ϕ and its asymmetric intensity distribution at $P=-45°$ and 45° is just what we observed in this experiment, so $M_{CD}\,M_{LB}$ is considered to be the model for PEM.

By considering the existence of the static phase retardation Δ_i in the PEM, its phase retardation can be expressed as [14]:

$$\phi = \Delta_i + \Delta_0 \sin(\omega t)\,, \tag{9}$$

where Δ_i, Δ_0 and ω are the static retardation, modulation amplitude and modulation frequency of the PEM, respectively. Since the temporal averaged intensity $\bar{I}_k$ can be defined as $\int_0^{2\pi/\omega} I_k dt/(2\pi)$ by averaging Eq. (8), we can prove that

$$\bar{I}_k = \int_0^{2\pi/\omega} I_{k4}\mathrm{d}t/(2\pi) = I_0[\cosh \mathrm{CD} - \sin(2P-2\theta)J_0(\Delta_0)] \tag{10}$$

where J_0 is the zero-order Bessel function. If the absolute value of the CD is less then 0.1 and $\Delta_i < 5°$, then $\bar{I}_k \approx I_0$ and one can use it to normalize the intensity. Using the three-intensity measurements [4], the following can be proven:

$$\tan(2\theta) = \frac{I_a - \cos 2P}{\sin 2P - I_b}; \tag{11}$$

$$\cos\phi = \frac{I_a^2 + I_b^2 - I_a\cos 2P - I_b \sin 2P}{-1 + I_a\cos 2P + I_b \sin 2P} \tag{12}$$

where

$$I_a = [2I(0) - I(\pi/3) - I(2\pi/3)]/(3\ \bar{I}_k); \tag{13}$$

$$I_b = \sqrt{3}[I(\pi/3) - I(2\pi/3)]/(3\ \bar{I}_k). \tag{14}$$

Using Eqs. (11) and (12), along with the normalized intensity, we can calculate the optical axis and phase retardation, respectively. The CD can be obtained by substituting ϕ and θ into Eq. (8). It is easy to prove that the output Stokes parameter can also be obtained by the same measurements; i.e., $S_o=1$; $S_1=I_a$; $S_2=I_b$; and $S_3=\pm\,(1-I_a^2-I_b^2)^{1/2}$.

3. Experiment

The optical properties of a PEM were investigated using a PSA polarimeter. Fig. 1 depicts the experimental setup. Light (L, from a He–Ne laser) passed through a polarizer whose azimuth angle was set to 45° and −45° with respect to the horizontal axis. The analyzer was mounted on a stepping motor controlled rotator, and three radiances were measured at the azimuth of the analyzer at 0°, 60° and 120°. The operating frequency of the PEM (Hinds PEM-90™) was 50.91 kHz and its modulation amplitude was set to 2.405 for $J_o(\Delta_o)=0$. A data acquisition system (NI PCI-6111) was used to acquire the temporal intensity with a sampling rate of 10 MHz. Two consecutive experiments were conducted by setting $P=45°$ and $P=-45°$ to measure its physical parameters and its output Stokes parameters.

4. Results and discussion

From Eq. (6), it is very easy to prove that if the PEM is a pure linear birefringence material, the averaged intensity should be a constant, I_o. However, the measured averaged intensity I_k which fluctuates more than 10% not only depicts a periodic modulation but also exhibits anti-symmetric distributions at $P=45°$ and $P=-45°$, as shown in Fig. 2. This non-constant distribution ofI_k indicates that the artifactual circular dichroism does couple with the birefringence in the PEM. Using Eqs. (8), (11) and (12), along with the normalized intensity, we calculated the optical axis, phase retardation and circular dichroism, which are illustrated in Figs. 3, 4 and 5, respectively. From these figures, we can conclude that the azimuth angle of the optical axis and circular dichroism approach to a constant, except around the singular points, i.e., ωt close to 0 and π. In these measurements, the averaged results for the azimuth angle of the optical axis and circular dichroism were $-0.20\pm0.09°$ and -0.066 ± 0.002, respectively. The modulation amplitude was 2.488 (0.396 λ), which was closer to the panel value, i.e., 0.383 λ, than what was obtained by Wang et al.'s [3] calibration. By substituting these values in the intensity distribution, such as shown by the line in Fig. 2, the periodic anti-symmetric

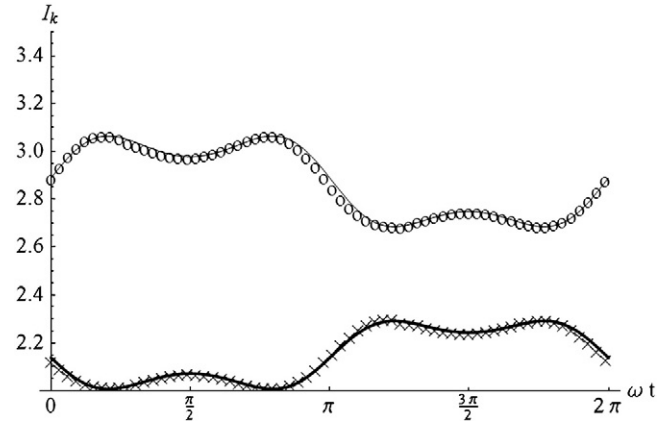

Fig. 2. The average temporal intensity distribution (I_k) measured at $P=45°(o)$ and $P=-45°(x)$. The lines show the theoretical distribution of I_k, where CD $=-0.066$, $\theta=0$ and $(\Delta_i,\Delta_0)=(0.076,2.488)$.

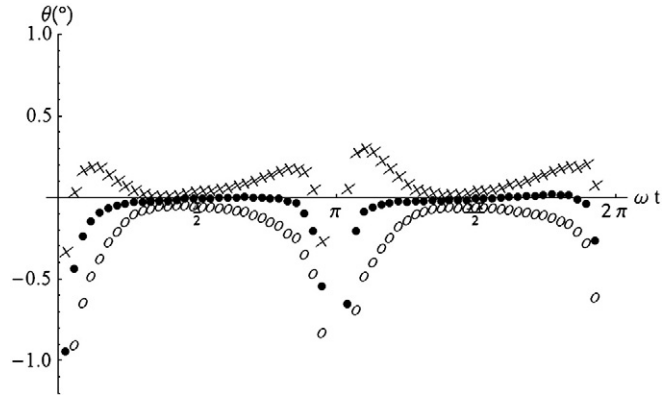

Fig. 3. The temporal azimuth distribution of the PEM's optical axis measured at $P=45°(o)$, $P=-45°(x)$ and its averaged (●).

distribution of intensity measured at $P=45°$ and $P=-45°$ can be explained.

The states of the polarization (SOP) of the light generated by the PEM can be applied in stroboscopic illumination imaging ellipsometry [13]. The precisely generated or measured SOP can be used to determine the success of the imaging ellipsometry. Since the SOP can be determined by the same three-intensity measurements, we like to compare the angular deviation (σ) of the SOP on Poincare sphere between the measured SOP (S_m) with that (S_a) of

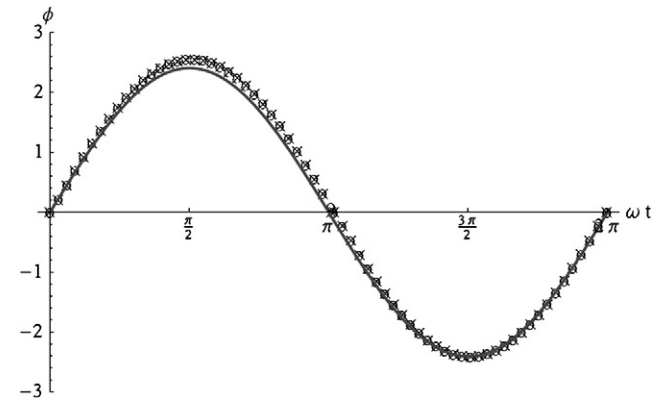

Fig. 4. The temporal retardation of the PEM: the line indicates its modulation amplitude $\Delta_o=2.405$; the measured retardation at P: $45°(o)$ and $-45°(x)$.

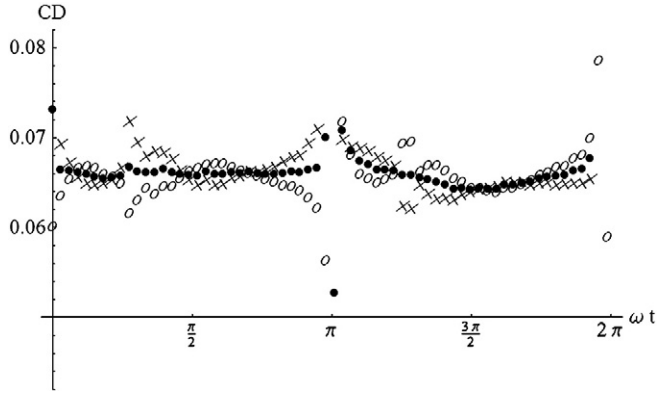

Fig. 5. The temporal CD distribution of the PEM measured at $P=45°(o)$, $P=-45°(x)$ and its averaged (●) values.

various models. Three models of PEM were simulated for comparison and noted as M_H, M_W and M_{CDLB}. The first one, M_H, is model of Hinds PEM-90, and its parameters (CD, Δ_i, Δ_o) are (0, 0, 2.405). M_W is model calibrated by Wang et al. [3], and its parameters (CD, Δ_i, Δ_o) are (0, 0.074, 2.526). And the last, M_{CDLB}, is model proposed in this paper, and its parameters (CD, Δ_i, Δ_o) are (−0.066, 0.076, 2.488). The angular deviation σ of these three models is illustrated in Fig. 6. Just as expected, the worst model is the one before calibration of Hinds PEM-90. After calibration, without considering the existence of CD, the angular deviation of the SOP is close to zero only in the first half period; the deviation in the other half can reach 4°. The angular deviations of the SOP of Model (III) are close to zero, except at the singular points. By comparison, we can conclude that the PEM is a linear birefringence medium followed by a weak CD medium.

The photoelastic modulator that employs the strain-induced birefringence can accompany with the unavoidable stray birefringence [15], such as static phase retardation, CD and dual modulation mode [16]. All these phenomena can only be analyzed from its waveform instead of its harmonic components which can bury all these effects in the Fourier transformation. The digitized oscilloscopic ability in data acquisition system indeed provides us a powerful tool to study the modulator for establishing some new instruments, such as stroboscopic illumination imaging ellipsometry [13] and Mueller Matrix polarimetry [17]. This work can quantitatively measure the artifactual CD effect of PEM and reduce its system error in CD spectrometer which consists with a PEM.

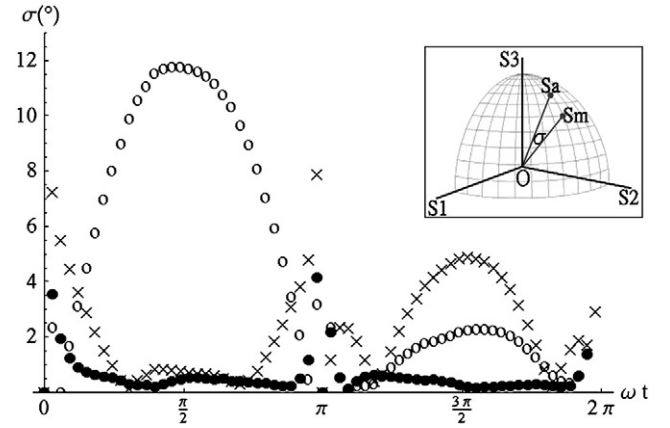

Fig. 6. The measured temporal SOP angular deviation (σ) on a Poincare sphere under various models of PEM (CD, Δ_i, Δ_o); Model (I) M_H, "o"; Model (II) M_W, "×"; Model (III) M_{CDLB}, "●". Upper right corner: angular deviation of σ on the Poincare sphere.

Acknowledgement

The authors acknowledge the funding from the National Science Council of Taiwan under the grant: NSC 98-2221-E-009-024.

Appendix

For anisotropic medium, Azzam and Bashara [18] listed the normalized Jones matrices in the followings:

$$J_{LB} = \begin{bmatrix} e^{j\frac{\phi}{2}} & 0 \\ 0 & e^{-j\frac{\phi}{2}} \end{bmatrix}, \tag{A1}$$

$$J_{LD} = \begin{bmatrix} e^{\frac{LD}{2}} & 0 \\ 0 & e^{-\frac{LD}{2}} \end{bmatrix} \tag{A2}$$

where ϕ and LD are the linear retardation and the relative attenuation, respective. The azimuth of fast axis and low-absorption axis are at zero, respectively. The circular attenuator with circular dichroism CD is written as

$$J_{LD} = \begin{bmatrix} \cosh(CD/2) & j\sinh(CD/2) \\ -j\sinh(CD/2) & \cosh(CD/2) \end{bmatrix} \tag{A3}$$

The Mueller matrix (M) can be transformed from its corresponding Jones Matrix by the unitary transformation [19],

$$M = U(J \otimes J^*)U^{-1}, \tag{A4}$$

where $\otimes$ represents the Kronecker product and U is

$$U = \frac{1}{\sqrt{2}} \begin{bmatrix} 1 & 0 & 0 & 1 \\ 1 & 0 & 0 & -1 \\ 0 & 1 & 1 & 0 \\ 0 & -j & j & 0 \end{bmatrix}. \tag{A5}$$

So, one can write the Mueller matrices for the linear retarder, linear and circular dichroism as

$$M_{LB} = \begin{bmatrix} 1 & 0 & 0 & 0 \\ 0 & 1 & 0 & 0 \\ 0 & 0 & \cos\phi & \sin\phi \\ 0 & 0 & -\sin\phi & \cos\phi \end{bmatrix}, \tag{A6}$$

$$M_{LD} = \begin{bmatrix} \cosh(LD) & \sinh(LD) & 0 & 0 \\ \sinh(LD) & \cosh(LD) & 0 & 0 \\ 0 & 0 & 1 & 0 \\ 0 & 0 & 0 & 1 \end{bmatrix}, \tag{A7}$$

$$M_{CD} = \begin{bmatrix} \cosh(CD) & 0 & 0 & \sinh(CD) \\ 0 & 1 & 0 & 0 \\ 0 & 0 & 1 & 0 \\ \sinh(CD) & 0 & 0 & \cosh(CD) \end{bmatrix}, \tag{A8}$$

References

[1] PEM-90 Photoelastic Modulator Systems User Manual, Hinds Instruments Inc, Hillsboro, Oreg., 1998
[2] J.C. Kemp, J. Opt. Soc. Am. 59 (1969) 950.
[3] M. Wang, Y. Chao, K. Leou, F. Tsai, T. Lin, S. Chen, Y. Liu, Jpn. J. Appl. Phys. 43 (2004) 827.
[4] Y.F. Chao, W.C. Lee, C.S. Hung, J.J. Lin, J. Phys. D Appl. Phys. 31 (1998) 1968.
[5] K. Claborn, E. Faucher, W. Kaminsky, B. Kahr, J. Am. Chem. Soc. 125 (2003) 14825.
[6] Y. Shindo, M. Nakagawa, Y. Ohmi, Appl. Spectrosc. 39 (1985) 860.
[7] B. Nordén, Å. Davidson, Acta Chem. Scand. 26 (1972) 1763.
[8] B. Nordén, Acta Chem. Scand. 27 (1973) 4021.
[9] J. Schellman, H.P. Jensen, Chem. Rev. 87 (1987) 1359.
[10] Y.F. Chao, K.Y. Lee, Jpn. J. Appl. Phys. 44 (2005) 1111.
[11] K.Y. Lee, Y.F. Chao, Jpn. J. Appl. Phys. 44 (2005) L1015.
[12] C.-Y. Han, Z.-Y. Lee, Y.-F. Chao, Appl. Opt. 48 (2009) 3139.
[13] C.-Y. Han, Y.-F. Chao, Rev. Sci. Instrum. 77 (2006) 023017.
[14] J. Badoz, M.P. Silverman, J.C. Canit, J. Opt. Soc. Am. A 7 (1990) 672.
[15] Å. Davidsson, B. Nordén, S. Seth, Chem. Phys. Lett. 70 (1980) 313.
[16] R. Petkovšek, F. Bammer, D. Schuöcker, J. Možina, Appl. Opt. 48 (2009) C86.
[17] Hsiu-Ming Tsai and Yu-Faye Chao, Opt. Lett. 34 (2009) 2279.
[18] R.M.A. Azzam, N.M. Bashara, Ellipsometry and Polarized Light, first ed., 1977 North Holland, Amsterdam.
[19] E.L. O'Neill, Introduction to Statistical Optics, first ed.Addison-Wesley, Reading, Mass., 1963